Using carbon dioxide for enhancing the permeability in deep geothermal carbonate aquifers

Alireza Arab and Broder Merkel
Technische Universität Bergakademie Freiberg

Abstract

Adequate permeability and favorable fluid pathways are vital aspects in geothermal energy production. But very often both criteria cannot be assumed as given. Also, due to scaling and precipitation, the worsening of permeability in different locations poses a challenge for deep carbonate dominated aquifers. Therefore, preserving and improving these pathways during long term operation is a key task in deep geothermal energy production.

With the aim of maintaining and enhancing the transmissivity of the fractures, the feasibility of adding CO_2 to the geothermal water was investigated. The interactions of the carbonate reservoir rock with water and CO_2 under reservoir conditions were investigated kinetically using rock cuttings from the Malm reservoir in Kirchweidach. Also, different materials which come into contact with CO_2 saturated water such as casing material and borehole cementation were tested under reservoir conditions for a predetermined period of time. The solution samples of all experiments were analyzed for their chemical composition (by means of ICP-MS and IC), as well as the content of the dissolved CO_2 in the water. In addition to the water chemistry analyses, a microscopic examination of solid material surfaces before and after the experiments was carried out on the sample material using SEM.

The results for the rock material show a preferred dissolution of major rock forming minerals caused by increased pCO_2. Respectively, the investigation of the casing material showed that it experienced a weight loss of 1.7% during the test period of 28 days and no indications of passivation on the casing surface were found. As for the concrete samples, results demonstrated that there is a weight gain of 5-10 weight%, which is associated with carbonation of the cement.

In parallel to the laboratory experiments, a pilot plant (bypass system) was used where cooled geothermal water from the Malm reservoir was enriched with CO_2. Then, the CO_2-enriched geothermal water passed through rock-filled columns, which were sequentially heated up to the reservoir temperature. During the 6 months operation period, redox potential in the inlet and outlet, EC, pH, flow, and temperature were monitored. Correspondingly, continuous sampling was done so that the main cations, DOC, and acid and base capacity ($Sk_{4.3}$, $Bk_{8.2}$) were analyzed. The bypass system which was used in this research allowed for flexible simulations of boundary conditions and tracking of the corresponding reactions during the reinjection of geothermal thermal water back into the aquifer.

Taken together, results show that adding CO_2 to the geothermal water can lead to a favored dissolution of the carbonate rock which could be used to enhance the permeability in low permeable carbonate reservoirs by using this natural gas. Also, precipitation of carbonate minerals and the formation of scales which deteriorate the transmissivity of reservoir pathways can be prevented due to under-saturation with respect to carbonates. Furthermore, this suggested approach could

eventually become a safer and resource-conserving alternative to current techniques especially due to the fact that above ground energy production is not interrupted while CO_2 is being added. This and the positive CO_2 storage as by-effect (Carbon Capture, Utilization and Storage) can be important factors for policymakers.

1. Introduction

Geothermal energy is considered as one of the alternative energy sources to fossil energy. In Germany, there are many regions which have considerable geothermal potential such as the Northern German Basin, the Upper Rhine Graben and the South German Molasse Basin (Schellschmidt et al. 2010). In the South German Molasse Basin, geothermal energy is extracted from open fracture systems and karst in the southern and central part of the Malm formation (Fritzer et al. 2010).

During geothermal production, the geochemical equilibrium between the carbonate reservoir rock and groundwater is disturbed because of temperature and pressure changes. This can lead to precipitation of scales on well pipe walls leading to clogging of wells, reducing injectivity, and damaging the pumping system. Besides, experience from existing plants in the region show that in addition to precipitation on pipe walls and heat exchanger surfaces, a suspension of carbonate crystals is formed. These crystals can precipitate inside the fractures and disturb the continuous production as well as causing technical damage. A small reduction in porosity due to precipitation can cause significant permeability reduction (Bacci et al. 2011). If there is not sufficient permeability or the permeability is reduced due to precipitation, heat cannot be exploited from the geothermal reservoir (Tester et al. 2007).

It is in this light that the addition of CO_2 to geothermal water was considered as an innovative way of enhancing permeability in low permeable aquifers and maintaining existing fractures and pathways. By increasing the partial pressure of CO_2 in water, the water becomes under-saturated with respect to calcite. This not only prevents carbonate precipitation but also triggers favorable carbonate dissolution. This dissolution will continue until the formation water is once again in equilibrium with the aquifer rock. As a result, even a small increase in porosity has significant effect on enhancement of permeability.

With the aim of long-term improvement and preservation of reservoir pathways in deep geothermal energy, our suggested technique was tested in the laboratory (batch experiments) and in a pilot plant (bypass system). In the batch experiments, the interactions of the reservoir rock with water and CO_2 under reservoir conditions were investigated kinetically. Also, different materials that come into contact with CO_2 saturated water during reinjection were tested under reservoir conditions for a predetermined period of time. As part of the LERWTG research project funded by the Federal Ministry of the Environment, Nature Conservation and Nuclear Safety and in cooperation with Hydroisotop GmbH, a bypass system was used to simulate and investigate the re-injection of cooled geothermal water with the addition of CO_2 on the reservoir rock. Over the duration of the testing period, different measurements and analyses were performed to determine rock-water-CO_2 interactions.

1.1 Kirchweidach- Molasse basin

Kirchweidach is a geothermal field designed for both electricity production and thermal use located in the Malm aquifer system of the Southern German Molasse basin. Kirchweidach is one of the most important reservoirs for geothermal energy production in the south due to its extensive fault system,

water-bearing nature at depth coupled with high permeability from partially karstified limestones and fractured dolomite at favorable temperatures (Seithel et al. 2015). According to Ganz et al. (2013), this progressive increment in temperature in the aquifer system, especially towards the Alps, makes areas on this part of the Malm formation potential sites for electricity generation. Most of the geothermal wells drilled here are mainly for heating and electricity production (Norden 2011).

2. Methodology

2.1 Sample material description

The sample materials used in the batch experiments consisted of rock cuttings from the injection well (GT1) and production well (GT2a), analog representative rocks and a drill core, steel well casing, and well concrete. In the bypass system (pilot plant), analog samples were used because the amount of drilling material would have been insufficient for filling the columns. The representative rock materials were taken from Ziegenfelder (Frankendolomite, Malm Delta), a quarry located in the same geological formation as the geothermal wells in Kirchweidach. XRD data based on qualitative and semi-quantitative analysis with the Rietveld method was performed on all the rock samples to obtain mineral compositions. The steel casing sample was analyzed by EDX. Table 1 lists a summary of the sample material used and their composition. Microscopic examination of samples was also carried out before and after some the experiments using SEM for possible changes to the surface of the material

Table 1: XRD (*EDX for steel) results for the sample material used in experiments

Sample	Dolomite wt%	Calcite wt%	Ankerite wt%	Quartz wt%	Experiment
GT1	68	26	4	-	Batch
GT2a	75	14	11	2	Batch
Analogue A1	96.21	3.41	-	0.39	Batch
Analogue A2	94	5.56	-	0.43	Bypass system
Analogue core B1	96.2	3.3	-	0.5	Batch
Steel casing*	Iron (98.65 wt%), manganese (0.9 wt%), silicon (0.25wt%), chrome (0.2wt%)				Batch

3.2 Batch experiments

Two different types of autoclaves (shown in figures 1 and 2) at a pressure of 40Mpa (400 bar) and a temperature of 105 °C were used to perform both batch kinetic and endpoint experiments. The kinetic experiments were done using GT1 and GT2 rock samples to investigate the effect of CO_2 on the reservoir rock and obtain the change of concentrations over time. The endpoint experiments were done to also determine the effect of CO_2 and water on the sample material (analog rock, drill core, steel casing and well concrete) after a predefined period, which was assumed to be sufficient to reach quasi equilibrium. Upon completion of all the experiments, the sampled solutions were tested for their chemical composition by means of ICP-MS and IC. The amount of CO_2 dissolved in the water was also measured in some experiments.
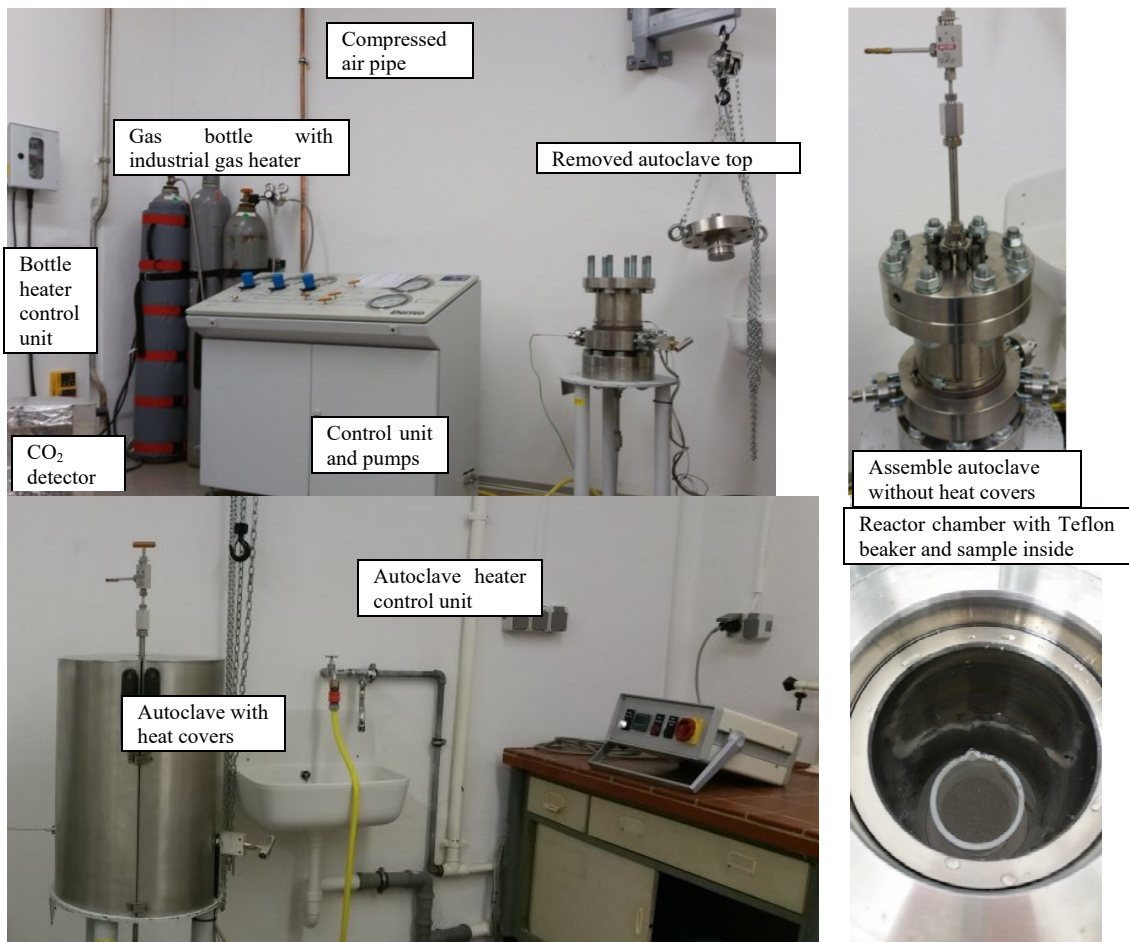
Fig. 1: Autoclave at TU Bergakademie Freiberg which was used for batch experiments.

Fig 2: Rocking hydrothermal autoclaves at GFZ Potsdam; fully assembled autoclave (left), the monitoring unit (center), and the confining pressure controller (right)

3.3 Bypass system

During the operation of the bypass system, thermal water was diverted from the pipeline of the geothermal plant and enriched with CO_2 before entering five cylinders (reaction columns) that were filled with analogue A2 rock samples. The water gradually heated up while going through the reaction columns and the test path. The actual scheme of the plant and bypass system are shown in Figure 3a while figure 3b shows one of the reaction columns before completion and the details of each of the columns are given in table 2. The bypass system was technically tested and optimized during a period of 3 months, and the actual experimental ran for 6 months.

The water flow in the plant was approximately 10 ml/s and the CO_2 inflow was adjusted to approximately 1.5 Nl/min. This amount of CO_2 corresponds to a gas content of 2500 Nml/l water and as a result, a pH value of 4.8 to 5.5 is achieved. The pore volume in the total system is 403 liters. Therefore, the thermal water had a residence time of 11.2 h in the reaction columns. The pressure in the bypass system was set to a range of 5 to 6 bar.

Fig. 3: (a) Bypass system in Kirschweidach and (b) Reaction columns while being set up

Table 2: Details of the reaction columns 1 to 5

Column	Temperature (°C)	Total Volume (l)	Rock Mass (Kg)	Pore Volume (Vol. %)
1	20	183	279	43
2	50	183	280	43
3	60	183	270	45
4	70	183	278	43
5	80	183	275	44

During the 6 month period, 20 sampling series on all rock columns as well as raw geothermal water were carried out, which resulted in a total of 143 individual samples. The following analyses were carried out on the sampled fluids from the raw geothermal water and the reaction columns:
• Main cations and anions and also fluoride, silicon, strontium, sulfide, iron, manganese, zinc.
• DOC and partly TIC

In addition to the sample analysis, on-site parameters were also measured. These measurements included: pH under plant pressure, specific electrical conductivity (EC), redox potential using PCB electrodes, temperature, pressure (online), and acid and base capacity ($Sk_{4.3}$ and $Bk_{8.2}$).

4. Results and discussions

4.1 Kinetic experiments

When taken out of the reactor, some of the particles showed a distinct change in color to brick red. SEM comparison of particles before and after the experiments showed noticeable changes to the surface and rounding of edges which in most cases indicate dissolution and weathering of the minerals. Figure 4 show SEM photos of dolomite, calcite, ankerite and quartz particles before (left) and after (right) the kinetic experiments.

The conductivity time course showed a rapid increase in the first hours for all experiments and rose from 1028 µS/cm (calculated conductivity of CO_2 saturated distilled water at the given P-T conditions) to 3000-3500 µS/cm. Subsequently, EC decreased to 1500 µS/cm during the second and third day of the experiments.

Similar to the EC measurements, the pH values started with a pH of 3.1 (calculated conductivity of CO_2 saturated distilled water at the given P-T conditions) and then rose very rapidly to values around pH 6, which are only continued in the further courses to about 6.5. A methodological problem that exists in such experiments is the measurement of pH, since there are no sensors which provide reliable in-situ values under the p/T conditions. Measurements of the pH after sampling are always associated with a spontaneous degassing, so the pH values determined in this way are up to 2 pH units above the in-situ pH values.

The time course for calcium, magnesium, iron, copper, and silicon concentrations is shown in figure 5. For calcium there is a sharp and rapid rise in the first hours of the experiments followed by a slow rise until reaching equilibrium. For the experiments containing rock cuttings from the injection well (E2 and E5), calcium concentration reaches 9.9 mmol/l after the first 24 hours while in experiments containing the rock cuttings from the injection well, calcium concentration is generally lower. This could be due to the fact that the GT1 sample contains more calcite than GT2a. In experiments E4 and E5, equilibrium is reached after 500 hours. In experiment E2, the equilibrium is reached before the 168th hour. As for experiment E3 and V015, equilibrium was not reached during the time which was set for the length of the experiment. The slight differences in the concentrations are probably due to the different characteristics of the respective cuttings.
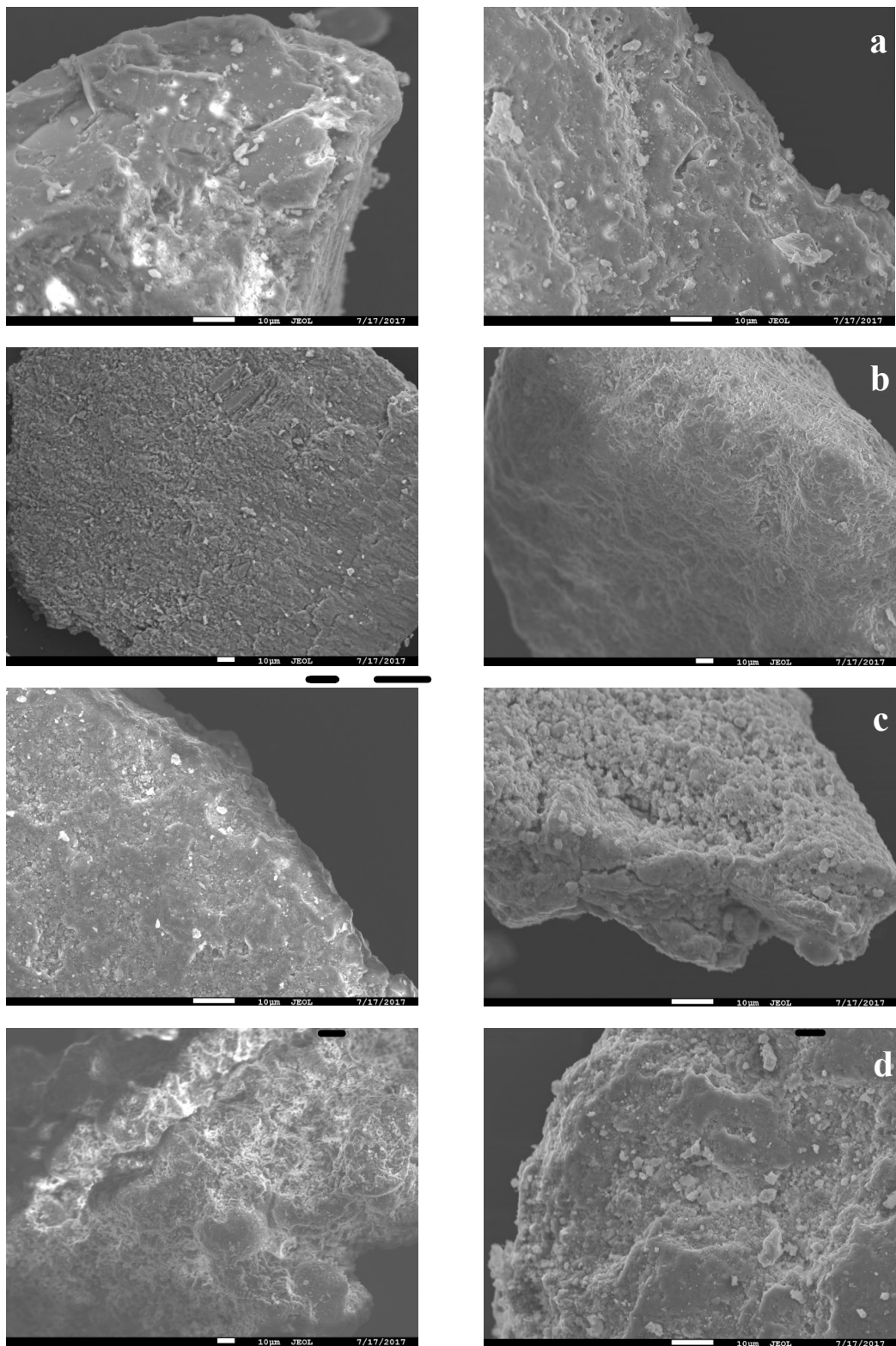
Fig. 4: SEM images before (left) and after (right) the kinetic experiments. (a) Shows distinct pits and holes have formed on the surface of the particle due to dissolution of dolomite. (b) Shows the changes to surface of calcite after the experiment; (c) is a corroded ankerite particle and (d) is the surface of a quartz particle after experiment which shows clear signs of dissolution as well as some attached precipitations.

Magnesium shows a similar behavior as calcium but at lower concentrations. There is a rapid increase in its concentration during the first hours for all experiments followed by a slower rise until equilibrium is reached. In experiments E2, E3 and E5, equilibrium is reached quicker for magnesium compared to calcium namely around 300 hours and even earlier. The dissolved magnesium concentration at equilibrium in experiments with the GT1 rock sample is twice the amount of experiments that contained the GT2a samples. This was not the case for calcium.

Manganese also shows similar behavior as calcium and magnesium. The manganese concentration after 500 hours in experiments with the GT1 samples is more than three times the samples of GT2a. Iron and copper show similar behavior over time but at different magnitudes. Iron concentration peaks to a maximum of 0.099 mmol/l in GT1 and 0.23 mmol/l in GT2a after 3 hours. Afterwards, iron concentrations very rapidly drop to 0.0085 mmol/l and even lower in all autoclave 1 experiments (E1 to E5) at around 70 hours. With the two samples of GT1, however, the iron concentration increases again after about 80 hours, while the two experiments, namely E3 and E4 that contain GT2a do not show this increase. Iron concentration in experiment V0105 also drops to below detection limit but it happens after 72 hours. It is also noticeable that the concentrations of iron in GT1 are significantly higher than in GT2a, although GT2a contains more ankerite.

For copper, in experiments E3, E4, and E5, a similar pattern for iron is observed with a rapid increase during the first 3 hours and then a rapid decrease to below 0.0018 mmol/l. However, in the experiment E5 which initially increases up to 0.058 mmol/l, it reaches 0.0013 after 500 hours. In experiments E1, E2, and V015 copper concentrations and the changes in concentration over time is very low.

Manganese also shows similar behavior as calcium and magnesium. The dissolved amount of manganese after 500 hours in experiments with the GT1 samples is more than three times the samples of GT2a.

With regard to the silicon concentrations, there is a clear difference between the cuttings of GT1 and GT2a where GT1 time course shows a significantly higher increase in silicon concentration. This is not surprising given the fact that the sample of GT1 has a higher amount of quartz content. Due to the slow kinetics of quartz, it was not expected that equilibrium would be reached in any of the experiments during the experimental period.
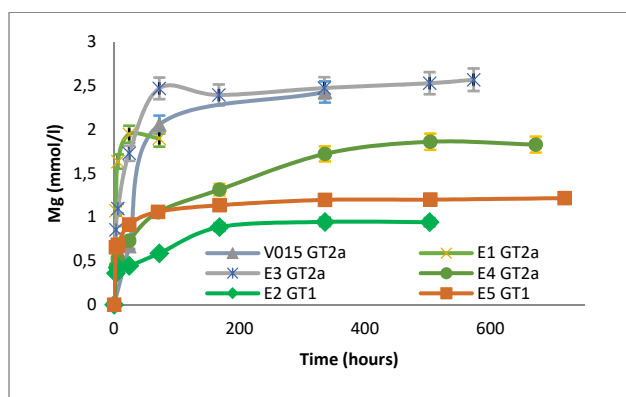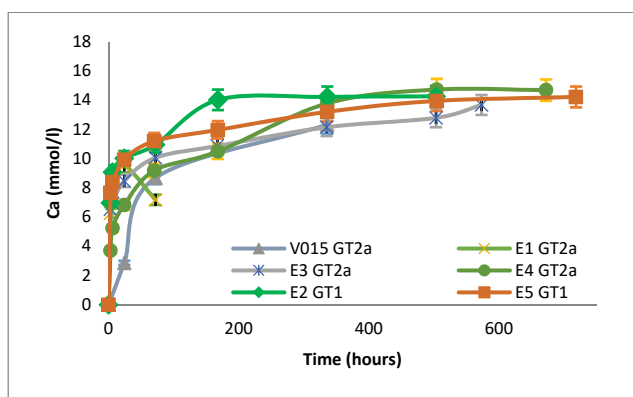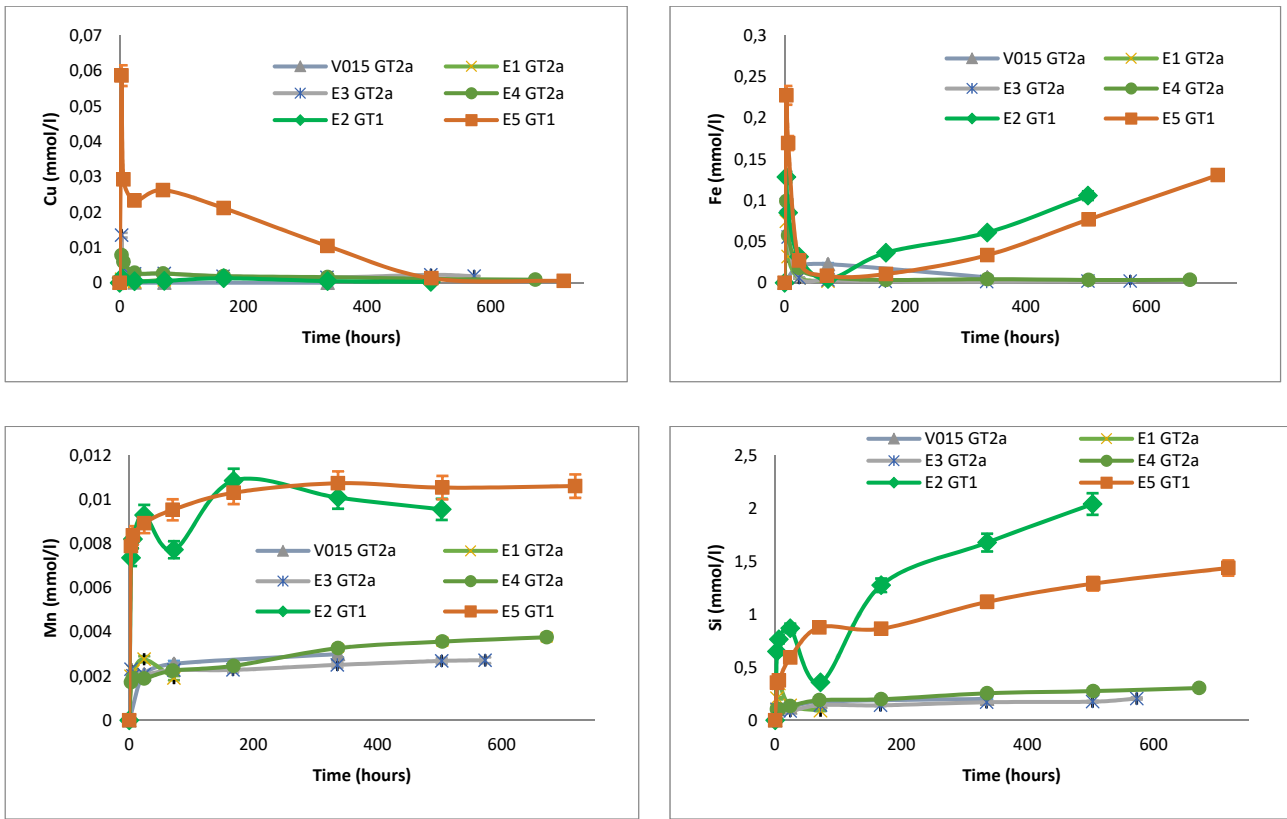
Fig. 5: Time series obtained from kinetic experiments for calcium, magnesium, iron, copper, manganese and silicon.

4.2 Endpoint experiments

4.2.1 Analog rock sample

SEM/EDX analysis was performed for the analog rock sample both before and after experiment. These images at different magnifications show clear signs of dissolution. Also, round sphere shaped particles could be seen which may perhaps be sorbed on the surface or precipitation due to change in the boundary conditions at the end of the experiments.
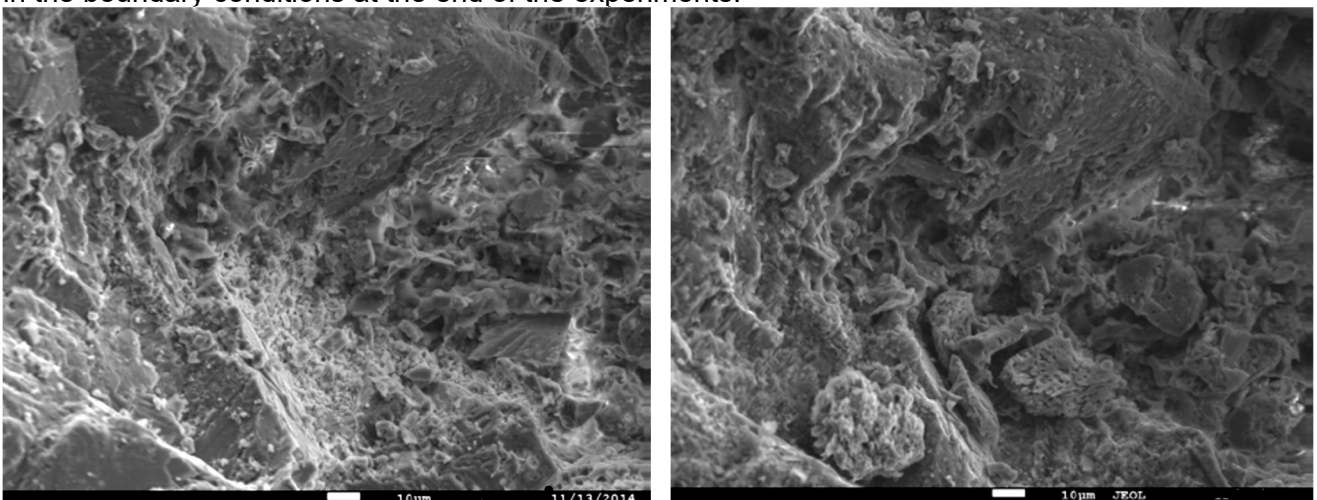

Fig 6: SEM images of the sample A1 before (left) and after (right) the endpoint experiment. Three points were selected and marked so that the same points could be compared exactly [Anne Kaulisky].

9

Two different locations on the sample were also chosen to be analyzed with EDX. Four and nine point measurements were carried out both before and after the experiment in the autoclave. Before the experiment, calcium content in the sample was about 28 wt%, 12.5 wt% magnesium, and 59 wt% oxygen. After the experiment, calcium is present at 26 wt%, magnesium 14 wt%, and oxygen at 58 wt%. These measured values are for the specific locations on the sample only and cannot be considered the average content for the whole sample. Nevertheless, it does indicate a mass change at the surface of the dolomite sample.

ICP-MS analysis results show that calcium has the highest concentration (33521 mg/kg rock) followed by magnesium (13420 mg/kg rock), sulfur (344.3 mg/kg rock) and silicon (120.9 mg/kg rock). Sodium, potassium, manganese, aluminum, strontium, zinc, iron and copper are distributed over a concentration range of 10 to 61 mg/kg rock.

4.2.2 Well cement sample

After removing the samples from the autoclave and drying it at 105 °C, white precipitates were observed on the concrete samples. These precipitates did not occur everywhere and were seen majorly on the lower part of the sample and were less towards the top of the specimen because all of the sample was not covered with water. In addition, a brownish change in the color of the concrete samples occurred. Figure 7 shows before-and-after pictures of the cement sample, on which change of the color and presence of the white precipitates are clearly shown.

Fig. 7: Concrete sample before (left) and after experiment (right) V012. Brownish discoloration and white precipitates on the concrete is clearly visible [Anne Kaulisky].

Samples were also weighed after the experiments. Both samples gained weight. The experiment was performed in duplicates and the samples were weighed with two different scales so that an error in the results could be put aside.

4.2.3 Analog drill core

Similar to the previous experiments, white precipitates were seen on the rock sample after it was dried at 105 °C. Further examination of the rock sample also showed clear signs of dissolution inside the fracture and voids. Three of such parts are shown by red markings in figure 8.

Fig. 8: Drill core sample before (left) and after (right) experiment. Clear signs of dissolution are visible on the edges of fractures and voids (red markings) [Anne Kaulisky].

A pH of 5.86 was measured immediately after sampling and the conductivity was 1700 µS/cm. The weight of the core after drying was 244.096 g. Thus 1.425 g of the rock has dissolved which corresponds to -0.58% (initial weight was 245.521 g). ICP-MS analysis showed that calcium had the highest concentration (1363 mg/kg rock), followed by magnesium (376.7 mg/kg rock), silicon (21.11 mg/kg rock), sulfur (15 mg/kg rock), potassium (10.99 mg/kg rock), and sodium (7.31 mg/kg rock).

4.2.3 Casing material

A change of color in the water and the white Teflon beaker is seen after opening the autoclave. Also, there is a noticeable brownish change in color on the lower part of the steel specimen and this fades upward until no change is visible at the top part (see figure 9). In addition, purple particles could be seen in the Teflon beaker as precipitates.

Fig 9: Casing material sample after experiment V012; red brown discoloration (probably iron oxide) is visible on the lower part [Anne Kaulisky].

The steel casing piece was 6.041 g after the experiment which indicates a weight loss of 0.104 g (6.145 g initial weight). This corresponds to a loss of 1.69 %. The water sample was also analyzed for its chemical composition by ICP-MS and IC. During the 28-day experiment, 6.931 g/kg of iron and 0.331 g/kg of manganese had been dissolved. Other alloying components were not identified.

4.3 Bypass system

During a period of 6 months, approximately 150 m³ of thermal water diverted to the bypass system. Approximately 385000 NL of CO_2 was added to the thermal water which yields to 17190 mol CO_2 (756 kg). A total of 1375 kg of rock was used in each cylinder. When 150 mg/l of calcite has been dissolved, therefore, a total of approximately 58 kg of $CaCO_3$ or 4.2% of the total rock is dissolved after 6 months. Table X shows the mass balance calculated for calcite and dolomite.

Table 3: Calcite and dolomite mass balance. vF1 is before the first rock (at the supply line) column and F1 to F5 are rock columns 1 to 5.

		vF1	F1	F2	F3	F4	F5
Average calcium concentration	(mg/l)	25	115.5	153.2	167.1	175.8	178.6
Increase of calcium content	(mg/l)	0	90.5	37.7	13.9	8.7	2.8
Increase in % of total increase	%	0	59%	25%	9%	6%	2%
Calcite dissolution	(kg)	0	35.4	14.7	5.4	3.4	1.1
Average magnesium concentration	(mg/l)	4	45.8	58.5	59.2	60.6	60.5
Increase of magnesium content	(mg/l)	41.8	12.7	0.7	1.4	-0.1	41.8
Increase in % of total increase	%	0	74%	22%	1%	2%	0%
Dolomite dissolution	(kg)	0	21.8	6.6	0.4	0.7	-0.1
Rock mass before experiment	(kg)		279	280	270	278	275
Dissolved mass	Wt.%		20	7.6	2.1	1.5	0.4

4.4 CO_2 utilization and storage by-effect

Interestingly, limited geological utilization and storing of CO_2 is a positive by-effect of the approach used in this research. Geological CO_2 sequestration refers to the storage of CO_2 underground in depleted oil and gas reservoirs, saline formations, or deep, un-mineable coal beds (CCS, carbon capture and storage). The aim of storage of carbon dioxide or other forms of carbon is to mitigate CO_2 emissions caused by fossil fuel usage. CO_2 via dissolution in formation water is one of the approaches used for solubility trapping of CO_2. If during actual geothermal energy production, as low as 0.1 moles of CO_2 is added to per liter of the water that is being re-injected back into the aquifer at a rate of 100 kg/s, around 14000 metric tons of CO_2 will be used per year. This CO_2 is dissolved in the geothermal water and there is no risk of the gas escaping to the surface. For scenarios of direct introduction of CO_2 inside of the aquifer, much higher amounts than the mentioned weight is used. Such a CO_2 storage by-effect (Carbon Capture, Utilization and Storage) requires no additional energy or equipment which adds economic and environmental benefits to the geothermal energy production.

5. Summary and Conclusions

An innovative method has been tested to enhance the permeability of carbonate reservoirs, prevent carbonate scaling and maintain existing pathways by means of adding CO_2 to the geothermal water. Various batch experiments (endpoint and kinetic) were performed and potential geochemical reactions and processes on different materials (rock cuttings, analogue rocks, drilling core, steel casing, and concrete) were investigated under reservoir conditions. Also, the adding of CO_2 to the geothermal water and it heating up inside the aquifer was simulated and analyzed using a bypass system (pilot plant).

Batch experiments showed that calcium and magnesium dissociated from all rock samples under the acidic conditions at pH values of about 3. This resulted in a mass loss of 1 to 5% by weight. Correspondingly, the widening of voids and fissures were observed in one of the experiments where a drilling core sample was used. The investigation of the casing material showed that the steel used experienced a weight loss of 1.7% during the test period of 28 days. Attempts for long-term behavior could not be carried out here, however, no indications were found that passivation of surfaces occurs. The investigation of concrete samples showed a weight gain of 5-10 wt% which is due to carbonation.

Kinetic autoclave tests showed that equilibrium was established for calcite and dolomite over a period of 200 to 500 hours. For other accompanying elements and impurities in the carbonates such as iron and copper, on the one hand, a very rapid dissolution and on the other hand, a very rapid precipitation of secondary minerals was observed. Therefore, an incongruent solution of these minerals could be assumed.

In the bypass system, 80 to 90 mmol/l of CO_2 was added to the cooled geothermal water and passed through rock-filled columns, which were sequentially heated up to reservoir temperature. As a result, dissolution of calcite and dolomite happened at low pH and low temperature, while at higher temperatures and pH dissolution of calcite was observed. There was no significant precipitation of calcite with a pCO_2 of 5 to 8 bar and temperatures of up to about 85 °C and at the end of the bypass route, the calcium concentrations approached equilibrium. Analysis for main ion contents and the secondary constituents showed that adding CO_2 or the change in the pH and temperature only causes changes in the lime-carbonic acid balance (calcium and magnesium content, DIC). Also, in the case of the secondary species, only a decrease in the dissolved sulfide occurred, which can be attributed to precipitations of iron sulfides and partly to outgassing.

The achieved results can be used for similar sites with similar mineralogy and heterogeneity. Likewise, the obtained results from the kinetic experiments can be employed to develop reliable models for prediction and planning in any similar geochemically conditions. Also, the bypass system which was used in this research is well-suited for flexible simulations of boundary conditions and tracking of the corresponding reactions of geothermal water leading to and inside of the aquifer.

This suggested approach could eventually become a safer and resource-conserving alternative to current techniques especially due to the fact that above ground energy production is not interrupted while CO_2 is being added. This and the positive CO_2 storage by-effect (carbon capture, utilization and storage) can be two of the important factors for policymakers. An important next step at this stage would be the actual injection of CO_2 into a reservoir in the area of an injection well or further into the aquifer in order to test the gentle stimulation of the rock matrix and existing carbonate systems in the technical scale and under real conditions.

Sources

Bacci, G., Korre, A., Durucan, S.: An experimental and numerical investigation into the impact of dissolution/precipitation mechanisms on CO2 injectivity in the wellbore and far field regions, International Journal of Greenhouse Gas Control 5, (2011), 579-588.

Fritzer, T., Settlers, E., Dorsch, K.: Bayerischer Geothermieatlas: Hydrothermale Energiegewinnung, Bavarian State Ministry for Economy. Infrastructure, Traffic and Technology, Munich (2010)

Ganz, Britta; Schellschmidt, Rüdiger; Schulz, Rüdiger; Sanner, Burkhard: Geothermal Energy Use in Germany. In *European Geothermal Congress 2013, Pisa, Italy, 3-7 June 2013*, (2013) pp. 1–16.

Norden, B. (Ed.) (2011): Geothermal Energy Utilization in Low-Enthalpy Sedimentary Environments. In *(Scientific Technical Report STR ; 11/06), Potsdam : Deutsches GeoForschungsZentrum GFZ*.

Schellschmidt, R., Sanner, B., Pester, S., Schulz R.: Geothermal energy use in Germany. Proceedings, World Geothermal Congress, Bali, Indonesia, 25–29 April (2010)

Seithel, Robin; Steiner, Ulrich; Müller, Birgit; Hecht, Christian; Kohl, Thomas (2015): Local stress anomaly in the Bavarian Molasse Basin. In *Geotherm Energy* 3 (1), p. 77. DOI: 10.1186/s40517-014-0023-z.

Tester, Jefferson W.; Anderson, Brian J.; Batchelor, Anthony S.; Blackwell, David D.; DiPippo, Ronald; Drake, Elisabeth M. et al. (2007): Impact of enhanced geothermal systems on US energy supply in the twenty-first century. In *Philosophical transactions. Series A, Mathematical, physical, and engineering sciences* 365 (1853), pp. 1057–1094. DOI: 10.1098/rsta.2006.1964.

Technische Universität Bergakademie Freiberg, Gustav-Zeunet-Str. 12, 09599, Freiberg, Germany. araba@geo.tu-freiberg.de, merkel@geo.tu-freiberg.de